Centrality dependence of bulk fireball properties in $\sqrt{s_{NN}} = 200$ GeV Au–Au collisions

Johann Rafelski
Department of Physics, University of Arizona, Tucson, Arizona 85721, USA

Jean Letessier
Laboratoire de Physique Théorique et Hautes Energies, Université Paris 7, 2 place Jussieu, F-75251 Cedex 05, France

Giorgio Torrieri
Department of Physics, McGill University, Montreal, QC H3A-2T8, Canada
(Received 19 December 2004; published 22 August 2005)

We explore the centrality dependence of the properties of the dense hadronic matter created in $\sqrt{s_{NN}} =$ 200 GeV Au-Au collisions at the Relativistic Heavy Ion Collider. Using the statistical hadronization model, we fit particle yields known for 11 centrality bins. We present the resulting model parameters, rapidity yields of physical quantities, and the physical properties of bulk matter at hadronization as function of centrality. We discuss the production of strangeness and entropy.

DOI: 10.1103/PhysRevC.72.024905 PACS number(s): 24.10.Pa, 13.60.Rj, 12.38.Mh, 25.75.−q

I. INTRODUCTION

The measurement of hadron rapidity yields at the Relativistic Heavy Ion Collider (RHIC) facilitates a study of the physical properties of the hadronic fireball at time of hadronization (i.e., when these particles are produced). The objective of this work is to understand the impact parameter (reaction volume) dependence of the fireball bulk properties. We search for a change of the reaction mechanism as function of centrality: if a new state of matter is formed in central and semi-central nuclear *AA* collisions, but not in *pp* reactions, one would naively expect a visible change in some physical bulk properties for a sufficiently small number of reaction participants.

We consider, at the top RHIC energy $\sqrt{s_{NN}} = 200$ GeV Au-Au, the 11 centrality bins in which the $\pi^{\pm}$, $K^{\pm}$, p, and $\bar{p}$ rapidity yields have been recently presented (see Tables I and VIII in Ref. [1]). These precise experimental results involving a full range of centrality motivate this effort. We wish to establish, at the high level of precision now available for the RHIC $\sqrt{s_{NN}} = 200$ GeV run, what a rapid change of the particle ratios such as K^+/π^+, K^-/π^- as function of centrality means both for the bulk physical properties of the fireball, and for the statistical hadronization model (SHM) parameters dependence on centrality.

These six particle rapidity yield results are complemented with STAR results for the ratios $K^*(892)/K^-$ [2] and ϕ/K^- [3]. Both $K^*(892)/K^-$ and ϕ/K^- do not show a significant centrality dependence, but we make an effort to account for any dependence in our analysis.

We considered the difference between STAR [3] and PHENIX [4] ϕ results. We illustrate the situation in Fig. 1 [5]. The lines show our best fit results to STAR (top panel), PHENIX (middle panel), and the combined data set (bottom panel). The integrated yields agree for the top two panels with those reported by the experimental collaborations. We note that the integrated yield derived from the combined data fit (bottom panel of Fig. 1), to all available 10% centrality ϕ yields, is not compatible with the PHENIX yield. This is so, because the evaluation of the integrated PHENIX ϕ yield depends on the lowest $m_\perp$ measured yield. This data point appears to be a 1.5 standard deviation (s.d.) low anomaly compared to the many STAR ϕ results available at low $m_\perp$. This possibly statistical fluctuation materially influences the total integrated PHENIX ϕ yield.

The ratio $K^*(892)/K^-$ anchors and confirms the chemical freeze-out temperature T, which is the only parameter on which this ratio depends. The ratio ϕ/K^- comprises a multi-strange particle and anchors and confirms the chemical conditions at freeze-out. For this reason use of these yield results is of essence to obtain the precision results we present here. However, in principle the resonance yields maybe significantly altered by post-hadronization processes [6–8], or their observable yield could be impacted by decay product rescattering [9].

The chemical non-equilibrium hadronization model describes the experimental data analyzed very well. Moreover, in this model, one expects near coincidence of the thermal and chemical freeze-out. In this limit, there is no post-hadronization resonance yield evolution or significant decay product rescattering. We have never come across the need for SHM adjustments of yields of the K^* resonance or ϕ. Therefore, we do not pursue the development of kinetic yield evolution models for these particles. The interested reader can follow up these developments in Refs. [6–8].

II. STATISTICAL HADRONIZATION MODELS AND STATISTICAL PARAMETERS

The statistical hadronization model is, by definition, a model of particle production in which the birth process of each particle fully saturates (maximizes) the quantum mechanical probability amplitude, and thus, the yields are determined by the appropriate integrals of the accessible phase space [10]. For a system subject to global dynamical evolution, such as

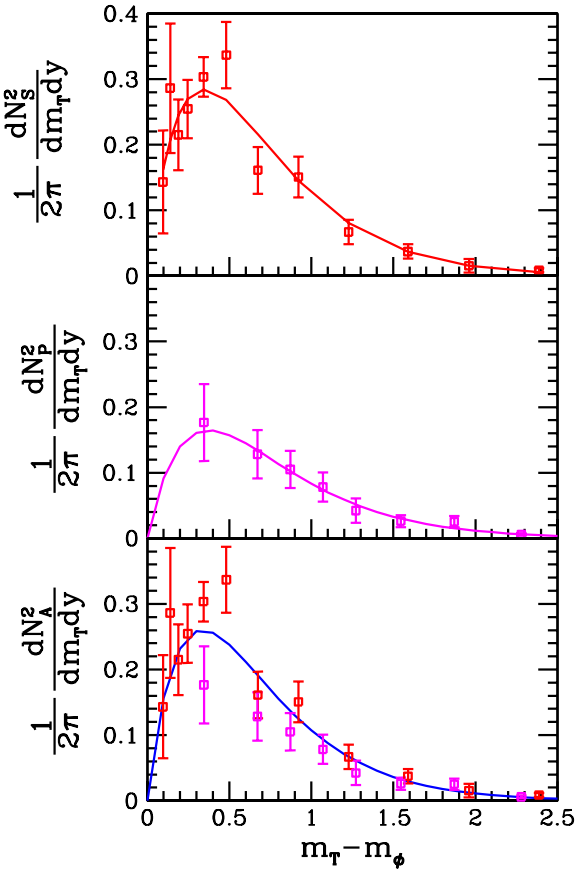

FIG. 1. (Color online) Measured ϕ-$m_\perp$ distributions $dN_i/dm_\perp dy$ for 10% most central collisions at $\sqrt{s_{NN}} = 200$ GeV, lines are best fits. (From top to bottom) STAR (subscript S), PHENIX (subscript P), and all data combined (subscript A).

collective flow, this is understood to apply within each local co-moving frame element. The results presented here were obtained using the numerical package SHARE (Statistical Hadronization with REsonances) [11].

The question, if SHM is indeed consistent with the wealth of RHIC data available today, comes to mind. Our comprehensive study of central reactions at central rapidity, for both $\sqrt{s_{NN}} =$ 130 and 200 GeV, suggests so strongly [12]. Systematic study of particle production for a wide reaction energy range confirms applicability of the SHM (for review see Ref. [13]). At RHIC there are two 2 s.d. exceptions among the model agreement with hadron particle yields at RHIC-200:

(i) The (preliminary) $\overline{\Omega}/\Omega = 1.01 \pm 0.08$ yield ratio [14], with the central value greater than unity, whereas on general grounds, at finite baryon density this ratio should be smaller than unity.
(ii) The (preliminary) $\Delta^{++}/p = 0.24 \pm 0.06$ [2,14,15], which in statistical hadronization models is half as large. We note that the central value of this result means that, after removal of descendants from weak decays, and assuming near isospin symmetry, nearly all protons observed should have been a primary Δ.

In addition to the eight particle (relative) yields considered, we also enforce three supplemental constraints:

(i) Strangeness conservation, i.e., the (grand canonical) count of s quarks in all hadrons equals such $\bar{s}$ count for each rapidity unit.
(ii) The electrical charge to net baryon ratio in the final state is the same as in the initial state to within 2%.
(iii) The ratio $\pi^+/\pi^- = 1. \pm 0.02$, which helps constrain the isospin symmetry.

This last ratio appears redundant, as we already independently use the yields of π^+ and π^-. These yields have a large systematic error and do not constrain their ratio well, and thus the supplemental constraint is introduced, because SHARE allows for the isospin asymmetry effect.

The successful description of particle yields within the SHM obtained for a single chemical freeze-out condition produces, as a first result, the model parameters in the process of χ^2 minimization: the (chemical) freeze-out temperature T, the baryon μ_B and hyperon μ_S chemical potentials. We obtain and present results at three chemical condition alternatives, the chemical equilibrium (dashed lines, red online), strange quark non-equilibrium with phase space occupancy $\gamma_s \neq 1$ (dotted lines, violet online), and the light quark flavor yield (full) non-equilibrium model including $\gamma_q \neq 1$ (solid lines, blue online). In our approach, 4 to 6 parameters confront, in a systematic fashion, 11 yields and/or ratios and/or constraints containing one redundancy.

The results we present for the model parameters, in Fig. 2, have all above 85% confidence level (we do not present the low centrality chemical equilibrium results as these do not satisfy this criterion). In Table I, we present all these results with precision that should help reproduce particle yields when required. In general, the reader should not expect to reproduce the last fourth digit shown. We also present, in Table I, along with A, and in same precision, the volume normalization factor dV/dy, which is required to obtain the particle yields. We further note that only one of the three models presented is applicable, and thus, the variation of parameters between these models must be seen as the sensitivity of the data to their physical relevance.

A notable feature, in Fig. 2, is absence of centrality features in temperature T and chemical potentials $\mu_{B,S}$, except for the most peripheral centrality and up to the variation that can be associated with fluctuation in the data sample and/or determination of the minimum of χ^2. The deviation, at the most peripheral centrality bin from trends set by other results, could be an indication of the change in the reaction mechanism for which we are looking.

Independent of the chemical (non-)equilibrium assumption, the baryochemical potential $\mu_B = 25 \pm 1$ MeV across the 10 centrality bins. Similarly, we find strangeness chemical potential $\mu_S = 5.5 \pm 0.5$ MeV (related to strange quark chemical potential $\mu_s = \mu_B/3 - \mu_S$). The freeze-out temperature is for the semi-equilibrium and equilibrium model about 10% greater than the full chemical non-equilibrium freeze-out. The most notable variation, in Fig. 2, is the gradual increase in strangeness phase-space occupancy γ_s/γ_q and thus

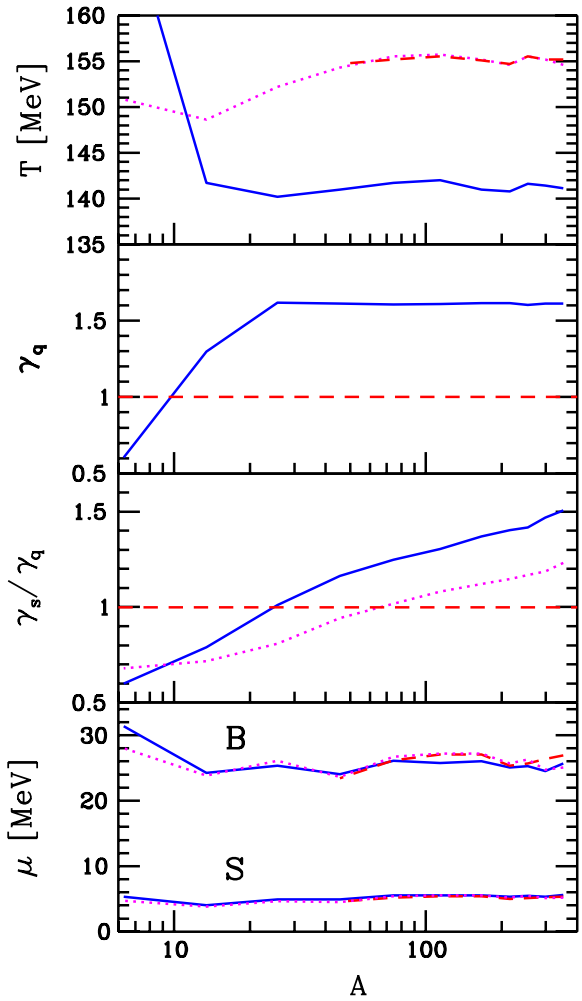

FIG. 2. (Color online) (From top to bottom) Temperature T, light quark phase-space occupancy γ_q, the ratio of strange to light quark phase-space occupancies γ_s/γ_q, and the chemical potentials (B for baryochemical μ_B and S for strangeness μ_S) as function of centrality (average participant number A). The lines connect the results obtained at each bin center A and have not been smoothed to show result fluctuations: (i) full chemical non-equilibrium model, (blue online) solid lines, (ii) strangeness chemical non-equilibrium model, (violet online) dotted lines, (iii) chemical equilibrium model, (red online) dashed lines.

strangeness yield with collision centrality. This effect was predicted and originates in an increasing lifespan of the fireball [16]. The over-saturation of the phase space has been also expected because of both the dynamics of expansion [17] and/or reduction in phase-space size as parton-based matter turns into HG [18]. This latter effect is also held responsible for the saturation of light quark phase space $\gamma_q \to e^{m_\pi/2T}$. A systematic increase of γ_s with collision centrality has been reported for several reaction energies [19].

Using SHARE, we find $T = 141 \pm 7$ MeV for non-equilibrium, and $T = 155 \pm 8$ MeV for the chemical equilibrium and strangeness non-equilibrium freeze-out. The error is our estimate of the propagation of the systematic data error, combined with the fit uncertainty; the reader should note that the error comparing centrality to centrality is negligible. This result for T is in mild disagreement (1.5 s.d.) with earlier chemical equilibrium fits [13,20]. This, we believe, is because of (i) differences in data sample used, specifically, the hadron resonance production results used provide a very strong constraint for the fitted temperature (ii) the more complete treatment by SHARE of hadron mass spectrum and of heavy resonances multi-particle decays.

We find two regimes of hadronization temperature as follows:

(i) For the chemical equilibrium case, and for the chemical semi-equilibrium case the hadronization temperature $T = 155 \pm 8$ MeV is right at the value of the cross-over temperature for lattice QCD with $2 + 1$ dynamical flavors results for $\mu_B \to 0$ in Refs. [21] and [22]. These two groups apply different methods and approximations; their results imply that at RHIC conditions the temperature of the cross-over from QGP to HG in chemical equilibrium is near to $T = 160 \pm 5$ MeV.

(ii) The chemical non-equilibrium model requires for internal consistency a fast hadronization process, for which the sole known mechanism is super cooling of the fireball because of rapid transverse expansion [23]. Supercooling implies that the hadronization temperature is below phase cross-over boundary, and the value $T = 141 \pm 7$ MeV, we have found in the full chemical non-equilibrium fit is a result internally consistent with this reaction mechanism. These issues are discussed further in the context of the search of phase threshold as function of reaction energy (see Ref. [12]).

For the chemical non-equilibrium sudden hadronization reaction picture, we further expect that the hadronization geometry is highly non-homogeneous, corresponding to, e.g., fingering breakup of the fireball. This makes it possible that the thermal and chemical freeze-out condition coincide [24,25], as the surface-to-volume area is large, emitted particles having a small probability to rescatter. For this reason, as noted before, there is no need to discuss changes in observable hadron resonance populations that may arise in post-hadronization scattering processes.

III. PHYSICAL PROPERTIES OF THE FIREBALL AT HADRONIZATION

Given the statistical parameters, we can evaluate the yields of particles not yet measured and obtain the rapidity yields of entropy, net baryon number, net strangeness, and thermal energy as function of centrality, shown in Fig. 3. We find, in the most central reaction bin, 14.9 ± 1.5 baryons per unit rapidity interval, a rather large baryon stopping in the central rapidity domain.

The entropy yield is reaching $dS/dy = 5000 \pm 500$. This compares to the estimate made recently by Pal and Pratt [26], who find $dS/dy = 4451 \pm 445$ for the most central 130 GeV reactions. One should note that the smoothness of the results, presented in Fig. 3 as function of A, is directly related to the smoothness of experimental data, which determines in some cases nearly directly these observables. For example, the hadron multiplicity per rapidity unit is directly related to the

TABLE I. Fitted statistical parameters for each central value of centrality expressed in terms of participant number A, as defined by PHENIX; for the three models in sequence: chemical non-equilibrium model, chemical semi-equilibrium, and chemical equilibrium.

A	dV/dy	T	μ_B	μ_S	λ_{I3}	γ_s	γ_q
351.4	969	141.1	25.67	5.592	0.9967	2.430	1.613
299.0	821	141.4	24.52	5.34	0.9969	2.367	1.612
253.9	706	141.6	25.27	5.463	0.9968	2.270	1.603
215.3	611	140.8	25.05	5.325	0.9969	2.266	1.615
166.6	462	141.0	26.01	5.523	0.9968	2.212	1.614
114.2	298	142.0	25.75	5.528	0.9968	2.096	1.608
74.4	192	141.7	26.14	5.518	0.9968	2.003	1.605
45.5	119	141.0	24.05	4.929	0.9972	1.876	1.613
25.7	68.1	140.2	25.32	4.953	0.9972	1.636	1.618
13.4	55.1	141.7	24.24	4.045	0.9970	1.026	1.299
6.3	42.6	172.7	31.39	5.356	0.9954	0.363	0.606
351.4	1735	154.6	25.04	5.161	0.9958	1.231	1
299.0	1458	155.2	24.73	5.110	0.9958	1.186	1
253.9	1215	155.5	26.29	5.441	0.9956	1.169	1
215.3	1072	154.6	25.68	5.206	0.9957	1.147	1
166.6	795	155.2	27.18	5.540	0.9955	1.121	1
114.2	521	155.7	27.21	5.555	0.9955	1.080	1
74.4	334	155.5	26.74	5.367	0.9956	1.018	1
45.5	241	152.6	21.62	3.972	0.9967	0.8906	1
25.7	131	152.2	26.12	4.661	0.9962	0.8076	1
13.4	74.9	148.6	23.82	3.821	0.9969	0.7163	1
6.3	34.7	150.8	28.00	4.681	0.9961	0.6788	1
351.4	1920	155.2	26.93	5.349	0.9956	1	1
299.0	1609	155.2	26.41	5.249	0.9957	1	1
253.9	1328	155.5	25.70	5.137	0.9958	1	1
215.3	1157	154.7	25.32	4.982	0.9959	1	1
166.6	855	155.1	27.06	5.369	0.9956	1	1
114.2	550	155.5	27.06	5.414	0.9956	1	1
74.4	342	155.2	26.15	5.200	0.9957	1	1

Note: For dV/dy the unit is cubic Femtometers, for T, μ_B, μ_S the unit is mega-electron volts, and all other quantities are dimensionless.

entropy yield. Thus, the experimental yield error of 10% is directly the error of entropy dS/dy. If instead, we constructed this error from partial errors in the statistical parameters, the implicit cancellations would be hard to realize. For this reason, we do not state these errors in Fig. 3; all these micro canonical quantities are directly relate to particle yields and their error is at 10% level.

Except for the chemical equilibrium model (which has a restricted centrality range of validity, for it fails to fit the peripheral collisions), the rise of strangeness yield with centrality is faster than the rise of baryon number yield: $(ds/dy)/(dB/dy) \equiv s/B$ is seen in the top panel of Fig. 4. For the most central reactions, we reach $s/B = 9.6 \pm 1$. We also note fluctuations in the trend of the results of the magnitude expected from the experimental data error.

The increase, with A, of per-baryon specific strangeness yield indicates presence of a production mechanism acting beyond the first collision dynamics. This new mechanism must benefit from the increased size, or more appropriately, increased lifespan of the larger reaction system. We have shown earlier that the thermal gluon fusion to strangeness will have just this behavior [16].

Although entropy production occurs predominantly during the initial parton thermalization phase, thermal strangeness production requires presence of thermal, mobile gluons, being driven by thermal gluon fusion [27]. Thus, strangeness production follows in time the entropy production and is strongest at the highest available temperature considering the strangeness mass threshold.

To understand this better, we show, in the bottom panel of Fig. 4, strangeness per entropy s/S, as function of centrality. We find a smooth transition from a flat peripheral behavior where $s/S \lesssim 0.02$, to a smoothly increasing s/S reaching $s/S \simeq 0.03$ for most central reactions. This rise, occurring for $A > 20$, indicates the onset of an additional strangeness production mechanism.

As the system size increases, the time span during which thermal strangeness production is effective increases, allowing strangeness to approach chemical equilibration in the parton phase. A back-of-envelope estimate of the ratio of s/S, in a chemically equilibrated parton plasma, yields the value seen in Fig. 4 for large A [12]. We thus understand the rise and magnitude of s/S ratio in terms of the expected reaction mechanisms in the deconfined phase and the chemical

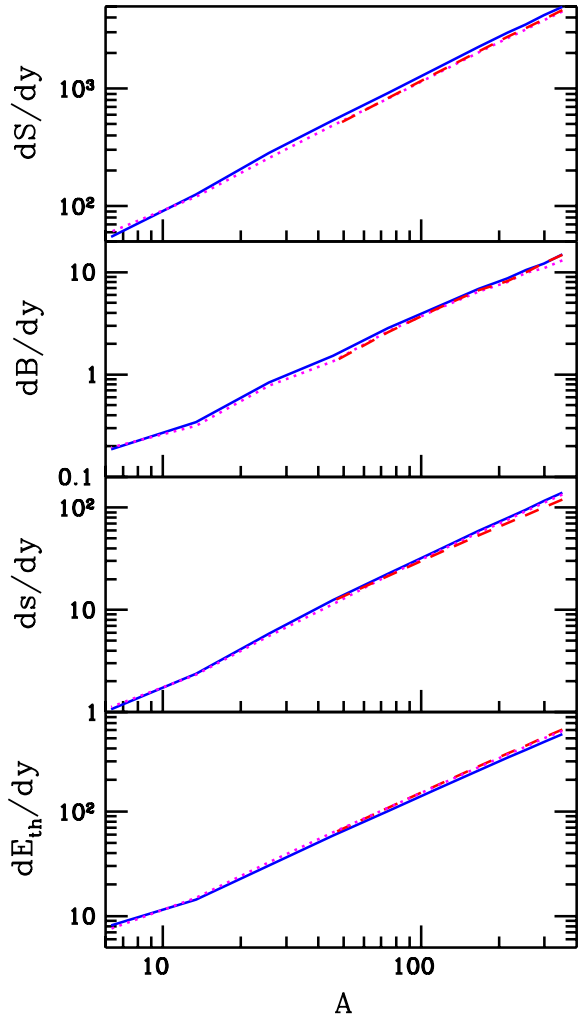

FIG. 3. (Color online) (From top to bottom) Entropy, net baryon, strangeness, and thermal energy yield per unit of rapidity as a function of centrality. Lines (nearly overlapping) are coded as in the legend to Fig. 2 for the three chemical models.

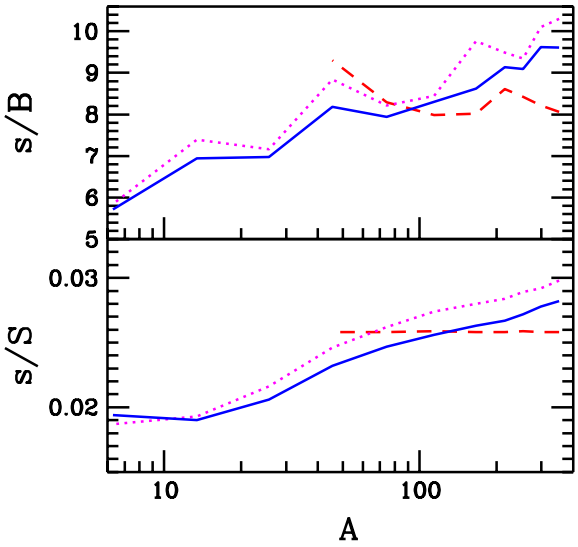

FIG. 4. (Color online) (Top) Strangeness per net baryon s/B and (bottom) strangeness per entropy s/S as a function of centrality. Lines are coded as in Fig. 2 for the three chemical models.

saturation of this ratio. Chemical saturation in QGP, i.e., $\gamma_s^{\rm QGP} \to 1$, implies, because of higher strangeness phase-space content in QGP than in hadron matter, that $\gamma_s > 1$.

We evaluate now the bulk properties of the fireball shown in Fig. 5. To obtain the pressure P, the energy density $\varepsilon \equiv (dE/dy)/(dV/dy)$ and the entropy density $\sigma \equiv (dS/dy)/(dV/dy)$, we sum, using the SHARE database for hadron resonances, all partial particle contributions using relativistic expression (see Ref. [10]). Because we fitted $6+2$ particle rapidity yields, the global fitted yield normalization factor $dV(A)/dy$ is reliable up to the systematic error of about 10% inherent in the PHENIX rapidity yield data.

When we consider ratios of two bulk properties, e.g., E/TS, the data and fit fluctuations cancel out, and the results are in general much smoother. Moreover, such ratios do not depend on the identification in the normalization factor dV/dy with the statistical model volume. For example, when one considers hadrons of finite proper volume [28], there is a correction factor. Hence, the smooth and precise values for E/TS that are not expected to be subject to model interpretation and will need to be addressed quantitatively. We note, as an example, that a quark matter system consisting of thermal mass quarks with $m = aT$, $a \simeq 2$ for non-equilibrium and $a = 4$ for equilibrium, will yield just the result seen in the bottom panel of Fig. 5.

We note, in Fig. 5, that the chemical non-equilibrium system is much denser at hadronization [29]. The entropy density, assuming chemical non-equilibrium, is by more than a factor of 2 larger compared to the chemical equilibrium model. It is for this reason that the ratio E/TS, in Fig. 5, is for the non-equilibrium case significantly smaller than it is when assuming equilibrium.

IV. FINAL REMARKS

We have presented a comprehensive analysis of soft hadron yields at $\sqrt{s_{NN}} = 200$ GeV as function of centrality. We have obtained the statistical hadronization parameters that describe the data and evaluated the physical properties of the hot fireball at hadronization. Our analysis included, aside of "stable" hadron PHENIX data ($\pi^{\pm}$, $K^{\pm}$, p, $\bar{p}$), also the STAR K^* and ϕ yields. For the latter, we also presented a comparison analysis to resolve a discrepancy between STAR and PHENIX ϕ-yield result. We found that, for $A \lesssim 20$, the statistical parameters do not vary with centrality, with the exception of strangeness quark occupancy, γ_s. Already for $A \gtrsim 20$, the system properties are approaching those seen for the greatest available $A \simeq 350$. However, for $A < 20$ there is a significant change in the physical and statistical properties of the fireball. The chemical equilibrium description of the experimental results here considered is not possible for these small fireballs.

We are aware of two prior efforts to explore statistical parameters, but not bulk properties, as function of collision centrality. At $\sqrt{s_{NN}} = 130$ GeV [30], the analysis remains

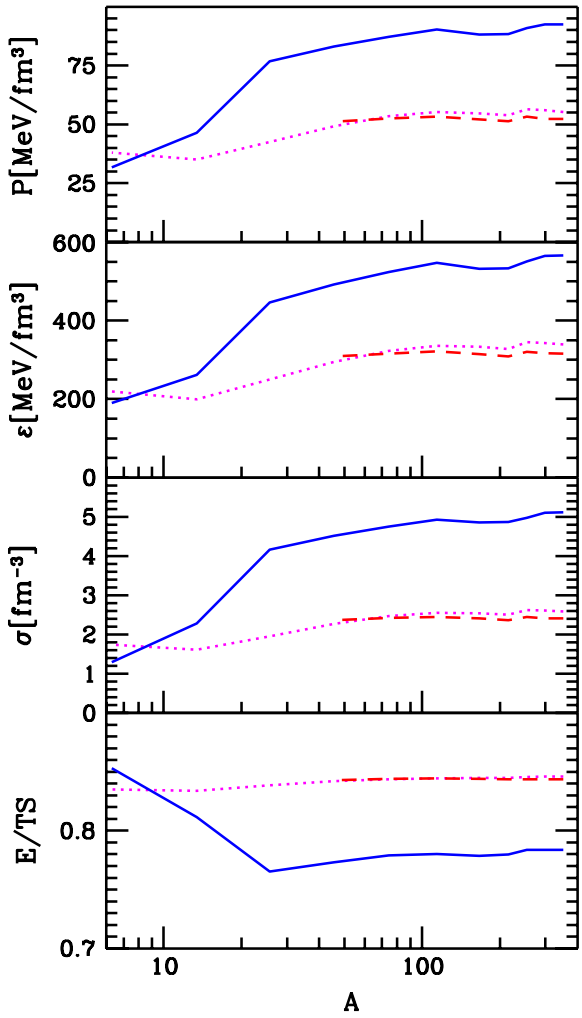

FIG. 5. (Color online) (From top to bottom) Pressure P, energy density $\epsilon = E/V$, entropy density S/V, and E/TS as a function of centrality. Lines are coded as in the legend to Fig. 2 for the three chemical models.

inconclusive in view of the limitations of the experimental data. At $\sqrt{s_{NN}} = 200$ GeV, an analysis assuming chemical semi-equilibrium [31] shows trends comparable with those we found. However, our hadronization temperature T and phase-space occupancy γ_s are anchored by the $K^*(892)$ and ϕ yields, and hence, we obtain for the chemical semi-equilibrium a smaller value of T and therefore a greater γ_s that for most central reactions clearly exceeds unity.

In this work, we have obtained the centrality dependence of the hadronization pressure, entropy density and thermal energy density, which are of the magnitude expected: for the chemical non-equilibrium model the pressure saturates at $P = 92$ MeV/fm^3, a typical value we are used to from the bag model of hadrons to be the vacuum pressure. The energy density of 0.5 GeV/fm^3 is in accord with lattice results for the energy density of matter subject to the phase transformation to/from deconfinement.

We have shown that the fireball strangeness content is increasing fastest with increasing centrality, out pacing in the competition both the stopped net baryon number and the produced entropy. We have shown that the ratio s/S saturates near the value of chemically equilibrated QGP phase.

In our opinion, the most remarkable finding of this study is the recognition that the statistical parameters, and thus also the bulk properties of dense matter fireball created at RHIC, do not depend on the size of the system for $A \gtrsim 20$, where A is the number of reaction participants. There is a rapid adjustment in the value of statistical parameters fitted: temperature is dropping and γ_q is increasing, which changes combine to yield a doubling in the density of the hadronizing fireball for $A \gtrsim 20$. Interpreting the high-density phase at hadronization as the deconfined state, our results can be interpreted to indicate that at the RHIC energy scale the quark liquid phase is formed for $A \gtrsim 20$.

ACKNOWLEDGMENTS

We thank Jingguo Ma and Zhangbu Xu for valuable comments, discussion, and the suggestion that the PHENIX ϕ-yield results are not inconsistent with STAR results when included in a common data analysis. Work supported by a grant from the U.S. Department of Energy DE-FG02-04ER41318, the Natural Sciences and Engineering research council of Canada, the Fonds Nature et Technologies of Quebec. LPTHE, Univ. Paris 6 et 7, is Unité mixte de Recherche du CNRS, UMR7589. G.T. thanks the Tomlinson foundation for support given.

[1] S. S. Adler *et al.* (PHENIX Collaboration), Phys. Rev. C **69**, 034909 (2004).
[2] H. B. Zhang (STAR Collaboration), in QM2004 proceedings (Oakland) (only at arXiv:nucl-ex/0403010); J. Adams (STAR Collaboration), Phys. Rev. C **71**, 064902 (2005)
[3] J. Adams *et al.* (STAR Collaboration), Phys. Lett. **B612**, 181 (2005).
[4] S. S. Adler *et al.* (PHENIX Collaboration), Phys. Rev. C **72**, 014903 (2005); D. Mukhopadhyay (PHENIX Collaboration), J. Phys. G **31**, S187 (2005).
[5] Jingguo Ma and Zhangbu Xu (private communication).
[6] M. Bleicher and H. Stocker, J. Phys. G **30**, S111 (2004).
[7] P. Fachini, J. Phys. G **30**, S735 (2004).
[8] Z. B. Xu, J. Phys. G **30**, S927 (2004).
[9] G. Torrieri and J. Rafelski, J. Phys. G **28**, 1911 (2002); J. Rafelski, J. Letessier, and G. Torrieri, Phys. Rev. C **64**, 054907 (2001) [Erratum-*ibid.* C **65**, 069902 (2002)].
[10] J. Letessier and J. Rafelski, Cambridge Monogr. Part. Phys. Nucl. Phys. Cosmol. **18**, 1 (2002).
[11] G. Torrieri, W. Broniowski, W. Florkowski, J. Letessier, and J. Rafelski, Comp. Phys. Com. **167**, 229 (2005).
[12] J. Letessier and J. Rafelski, "Hadron production and phase changes in relativistic heavy ion collisions," (arXiv:nucl-th/0504028).
[13] P. Braun-Munzinger, K. Redlich, and J. Stachel, in *Quark Gluon Plasma 3*, edited by R. C. Hwa and Xin-Nian Wang (World

Scientific Publishing, Singapore, 2004), p. 491, and references therein.
[14] O. Barannikova (STAR Collaboration), "Probing collision dynamics at RHIC" (only at arXiv:nucl-ex/0403014), and references therein.
[15] C. Markert (STAR Collaboration), J. Phys. G **30**, S1313 (2004).
[16] J. Letessier, A. Tounsi, and J. Rafelski, Phys. Lett. **B389**, 586 (1996).
[17] J. Rafelski and J. Letessier, Phys. Lett. **B469**, 12 (1999).
[18] J. Rafelski and J. Letessier, Nucl. Phys. **A702**, 304 (2002).
[19] B. Kampfer, J. Cleymans, P. Steinberg, and S. Wheaton, Heavy Ion Phys. **21**, 207 (2004).
[20] W. Broniowski, W. Florkowski, and B. Hiller, Phys. Rev. C **68**, 034911 (2003).
[21] F. Karsch, E. Laermann, and A. Peikert, Phys. Lett. **B478**, 447 (2000).
[22] Z. Fodor and S. D. Katz, J. High Energy Phys. 04 (2004) 050.
[23] J. Rafelski and J. Letessier, Phys. Rev. Lett. **85**, 4695 (2000).
[24] G. Torrieri and J. Rafelski, New J. Phys. **3**, 12 (2001).
[25] W. Broniowski and W. Florkowski, Phys. Rev. Lett. **87**, 272302 (2001).
[26] S. Pal and S. Pratt, Phys. Lett. **B578**, 310 (2004).
[27] J. Rafelski and B. Muller, Phys. Rev. Lett. **48**, 1066 (1982) [Erratum-*ibid.* **56**, 2334 (1986)].
[28] R. Hagedorn and J. Rafelski, Phys. Lett. **B97**, 136 (1980).
[29] G. Torrieri and J. Rafelski, J. Phys. Conf. Ser. **5**, 246 (2005).
[30] J. Cleymans, B. Kampfer, M. Kaneta, S. Wheaton, and N. Xu, Phys. Rev. C **71**, 054901 (2005).
[31] M. Kaneta and N. Xu, "Centrality dependence of chemical freeze-out in Au+Au collisions at RHIC," presented at QM2004 (Oakland) (only at arXiv:nucl-th/0405068).